Hylleraas hydride binding energy: diatomic electron affinities

Hylleraas hydride binding energy: Diatomic electron affinities

Edward S. Chen[1, 2], Herman Keith[2], Tristan Lim[2], Dang Pham[2], Reece Rosenthal[2], Charles Herder[2,3], Sunil Pai[2,4], R. A. Flores[5,6], Edward C. M. Chen [2,5]

1. Baylor College of Medicine, One Baylor Plaza, Houston Tx, 77030 *eschen@bcm.edu*
2. Wentworth Foundation, 4039 Drummond, Houston Tx, 77025 hkeith@comcast.net, tlimthai1996@gmail.com, dang.c.pham@hotmail.com reece.rosenthal@kinkaid.org,
3. *Current address: Massachusetts Institute of Technology Massachusetts Institute of Technology, 77 Massachusetts Avenue, Cambridge, MA 02139-4307, USA, cherder@mit.edu*
4. Current address Stanford University paisunil@yahoo.com
5. University of Houston Clear Lake, 2700 Bay Area Blvd Houston Tx, 77058, *Edward.chen@rice.edu*
6. Current address US EPA Region 6:10625 Fallstone Rd. Houston, TX 77099-4303 flores.raymond@epa.gov

Abstract: Theoretical adiabatic electron affinities are often considered inaccurate because they are referenced to only a single value. Ground state electron affinities for all the main group elements and homonuclear diatomics were recently identified using the normalized binding energy of the hydrogen atom; [0.75420375(3)/2 = 0.37710187(1) eV]. Here we revisit experimental values and extend the identifications to diatomics in the G2-1 set. We assign new ground state electron affinities: (eV) Cl_2, 3.2(2); Br_2, 2.87(14); CH, 2.1(2); H_2, 0.6 ; NH, 1.1, SiH, 1.90. Anion Morse potentials are calculated for H_2 and N_2 from positive electron affinities and for hyperfine superoxide states for the first time.

1.0 Introduction:

Theoretical adiabatic electron affinities, gs-AE_a, are incorrectly characterized because they are compared to only one benchmark. For example, the density functional AE_a : (eV) O_2, 1.08, 1.06, 0.62, 0.65, 0.35; NO, 0.97, 0.96, 0.53, 0.52, 0.43, 0.36; SF_6, 1.67, 2.66, 2.83, 2.85, 3.00, 3.22 in a frequently cited review, 2002R, were considered inaccurate, with an average deviation of 0.75 eV, when compared to AE_a : (eV) O_2, 0.451(7); NO, 0.026(5), SF_6, 1.07(7). The National Institute of Standards and Technology database, exp-NIST, cites experimental AE_a: (eV) O_2, 1.1, 0.725, 0.45, 0.33, 0.15; NO, 0.93, 0.85, 0.1, 0.026; SF_6 2.6(2),1.49(22), 1.07(7), 0.75(10), 0.54205, 0.32(15) while a 1953 review, 1953R, assigned the swarm and reduction potential, ERED, $AE_a(O_2)$, about 1 eV to the ground state and the swarm and Born Haber 0.77, 0.57, 0.33 eV to excited states. [1-5] The $AE_a(AB)$ is the energy difference between anions and neutrals in their geometries; Vertical E_a; VE_a in the neutral geometry and vertical detachment energy E_{vd} in the anion geometry.

In 1950, Massey stated: "The number of bound quantum states of a negative ion is not infinite. Indeed the small binding energy of the unattached electron in its ground state makes it unlikely that, apart from fine and hyperfine structure levels, ANY excited states will exist". [6] Two decades later, Lesk demonstrated all atomic E_a are positive and Efimov proved that three body quantum systems support an infinite number of bound states. Hydride, H(+) + 2e(-), is the simplest three body anion. [7,8] The normalized gs-E_a(H), designated the Hylleraas Hyl = gs-E_a(H)/2, = 0.75420375(3)/2 = 0.3771 eV/electron; the N_{Hyl} = gs-E_a(Z)/Hyl; the Rec = N_{Hyl}/N_v and dN_{Hyl} = [gs-$AE_a(Z_2)$ -gs-E_a(Z)]/ Hyl = [$D_e(Z_2[-])$-$D_e(Z_2)$]/Hyl were used to report positive gs-AE_a (Z & Z_2). The Rec: He-Rn, 0.2-0.3; Li-Fr, 0.82-0.63; B-Tl. 0.19-0.25; C-Pb, 0.67-0.58; N-Bi, 0.33-0.42; O-Te, 0.55-0.75; F-I, 1.13-1.02 illustrate the consistent periodicity. The density functional AE_a(N), 0.75 eV, the $AE_a(N_2)$, 0.6 eV from dN_{Hyl}, -0.5, and the $AE_a(H_2)$, 0.38 eV from dN_{Hyl}, -1 were assigned to the ground states. [9-14]

Electron correlation rules predict 54 superoxide states dissociating to [^{3}O + ^{2}O(-)] and 87 NO(-) states dissociating to [^{1}N + ^{2}O(-)] and [^{3}N(-) + ^{3}O]. [15] In 2004, Herder measured the temperature dependence of pulsed discharge electron capture detector, PDECD responses that gave $AE_a(O_2)$, 0.05 to 0.75 eV; assigned peaks at $AE_a(O_2)$, 0.05 to 1.07 eV, in the negative ion photoelectron spectra, NPES-95 to predicted states and applied the semi-empirical multi configuration configuration interaction CURES-EC, (**C**onfiguration Interaction, **U**nrestricted or **R**estricted **E**stimates of **S**elf consistent field **E**lectron **C**orrelation) method to account for the electron correlation problem, to superoxide, NO(-) and SF_6(-). [1,2, 16-21] In 2007, Toader and Graham characterized long range superoxide states observed in low temperature discharges using a semi-classical model. [22] The peak at 0.05 eV in the NPES-95 is now assigned to long range Efimov states. In 2010, Pai reported 27 bonding $AE_a(O_2)$, 0.15 to 1.07 eV from cyclic voltamagrams (CV). [23, 24] The Herschbach Ionic Morse Person Electron Curves, HIMPEC in Fig 1 were calculated from these values and negative values from $AE_a = 0.377dN_{Hyl} + AE_a$ (Z). [1, 14, 25, 26]

This work revisits and extends the methods used to report the gs-electron affinities of the main group atoms and homonuclear diatomics, O_2, NO, and SF_6. [1, 2, 14-24, 27-49] The NPES-02 was used as a prototype for the determination of the benchmark $AE_a(O_2)$ in 2002R. Here the 54 transitions from the 27 superoxide states to the two lowest neutral states are identified by comparison with the higher resolution NPES-95 and imaging spectra, IPES-10. [20,27] Hyperfine superoxide states are identified in experimental data. [1, 14-18, 21-24, 33] The theoretical E_a(Be & Mg), 0.28 eV, the largest evaluated experimental AE_a: (eV) Cl_2, 3.2(2), Br_2, 2.87(14), CH, 2.1(2); AE_a : (eV) H_2, 0.6, NH, 1.1, SiH, 1.9 estimated from dN_{Hyl} are assigned to the ground states. The dissociation energies for all of the diatomic anions are reproduced by semi-empirical anion Morse potentials, s-AMP. New HIMPEC for H_2 (-), N_2(-) and hyperfine O_2(-), are calculated using these data.

2.0 Experimental and theoretical methods

The literature data are obtained from tables or by electronic digitization of figures in the original articles. Any sources not specifically cited are from NIST, the 2002R or the 1953R. Shown in figure 1 are: ECD data for NO and O_2 from a dissertation by Freeman; other ECD, PDECD; atmospheric pressure negative ion mass spectral, API-NIMS data published in 2003 and 2013 and ECD, swarm, magnetron and flame data for O_2. These data and others were combined to report 27 $AE_a(O_2)$: (eV) X $^2\Pi$, [1.070,1.050]; $A^2\Delta$, [0.595, 0.562] ; B $^2\Sigma$, 0.515 ; C $^2\Pi$ [0.450, 0.430] ; D $^2\Sigma$, 0.415; E $^2\Sigma$, 0.360; a $^4\Sigma$ [0.950, 0.930]; b $^4\Delta$ [0.786, 0.750, 0.722, 0.702]; c $^4\Sigma$ [0.750, 0.730]; d $^4\Pi$ [0.312, 0.284, 0.264, 0.252]; e $^4\Sigma$ [0.250, 0.230]; f $^4\Pi$ [0.212, 0.180, 0.160, 0.148] used to estimate 27 negative values in Table 1. Also determined were $AE_a(NO)$: (eV) X $^3\Sigma$, 0.92; a $^1\Sigma$,0.40; b $^3\Delta$, 0.16 for states dissociating to N + O(-). These values and values for states dissociating to N(-) + O are compared to CURES-EC values in Table 2. The thermal values are from magnetron, ECD and swarm data.

Herder used the PDECD and chromatograph in Fig. 2 to measure the temperature dependence of high purity samples of O_2 as described in 2004. "Initial studies were carried out with helium as a carrier gas and Xe and Kr as dopants to obtain the simplest reaction composition. Studies were also carried out using more complicated dopants: synthetic air, O_2, and H_2. Samples were pure O_2 and synthetic air. " The AE_a and E_1 for NO and O_2 were determined by iterated least squares fits to: $K_{ex}= k_1/(2(k_{-1} + A_N))$: where K_{ex} is the molar response; A_N is the pseudo first order rate constant for anion losses; $k_1 = A_1T^{-1/2}\exp(-E_1/RT)$, $k_{-1} = A_{-1}T\exp(-E_{-1}/RT)$ are the electron attachment and detachment rate constants. The maximum A_1 from the DeBroglie wavelength of the electron is attenuated by the different third bodies. The A_{-1} is from: $K_{eq} = [(Q_{an}S_{an})(A_1/A_{-1})T^{-3/2}]\exp(E_a/RT)$ where Q_{an} and S_{an} are partition function and spin ratios. [1,2,14-21]

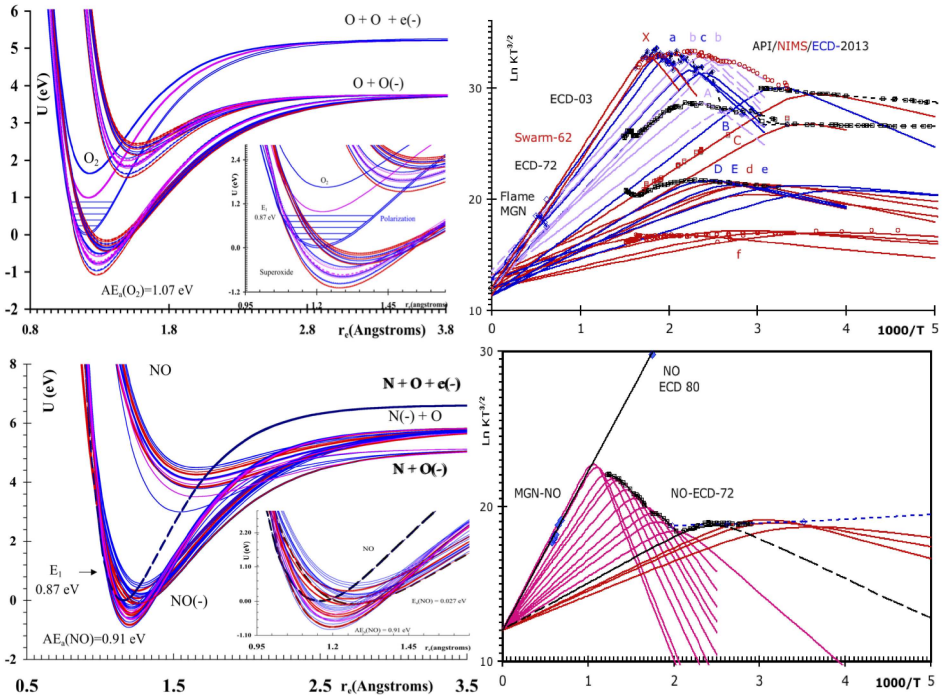

Figure 1: Neutral and anionic one dimensional Morse potential energy curves of energy vs internuclear separation referenced to the neutral dissociation energy = 0 and thermal data for NO and O_2 plotted as Ln $KT^{3/2}$ vs 1000/T from refs. 14-18,21,31,32,41,42.

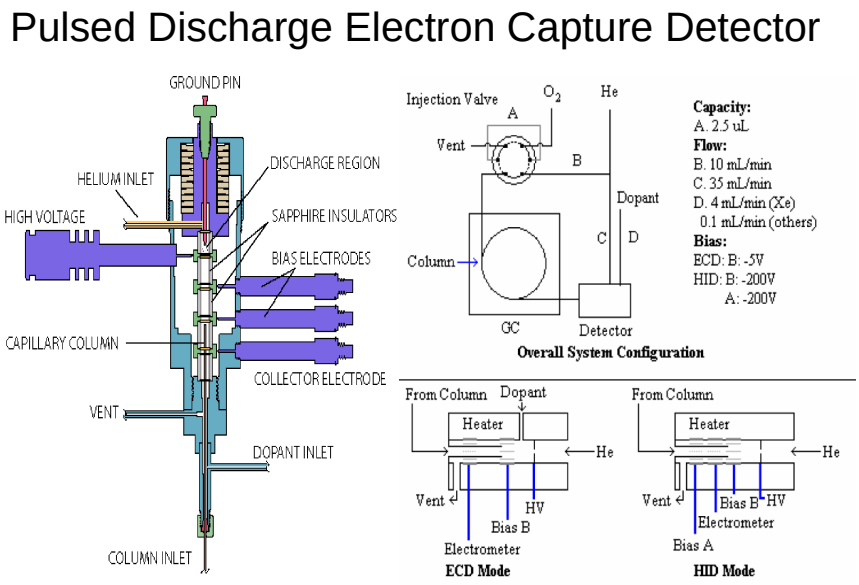

Figure 2: PDECD equipment used by Herder in 2004 from refs. 2,17,21

In 2008, Pai collected the electrochemical data shown in figures 3 and 5 and determined the 27 valence state $AE_a(O_2)$. He wrote, "The cyclic voltammograms of air-saturated solutions in dimethyl sulfoxide were recorded from T = 298K to 409K. The temperature was the only quantity changed. The reference electrode was a saturated calomel electrode stored in saturated KCl [Hg_2Cl_2]; the auxiliary electrode was platinum, and the working electrode was glassy carbon coated with functionalized multi-walled carbon nanotubes grown using chemical vapor deposition." Similar lower resolution data were obtained using standard glassy carbon electrodes. [23,24]

Herder matched all of the AE_a for NO as shown in Table 2 but only values for O_2 up to PM3(7100), 0.68 eV with CURES-EC described as follows. "The first step in the semi-empirical CURES-EC method is the selection of an E_a such as the experimental $AE_a(NO)$: (eV) 0.85(5), 0.68(20), 0.1(1), 0.0260(5). Then, geometry optimization SCF and MCCI, calculations are performed on the neutral and negative ion, for example PM3(aann), where a and n are anion and neutral filled and unfilled orbitals. The maximum E_a is the RHF(aa00), or the UHF (UU00) and the minimum RHF (00nn) where a and n are the maximum values. The optimum MCCI configuration is obtained by minimizing $\delta = abs(E_a(exp) - E_a)$. A successful calculation gives deviations less than the experimental uncertainty." [1,2,14-21]

The semi-empirical anion Morse Potential s-AMP method uses a subroutine in the HYPERCHEM suite to calculate dissociation energies of anions. In 2010, Pai reproduced the anion dissociation energy for the gs-$AE_a(O_2)$, 1.07 eV with the PM3(7100) s-AMP method. The $AE_a(O)$, 1.0 eV from the dissociation limit is 0.46 eV lower than the experimental values. Lim, Rosenthal and Pham applied the CURES-EC and s-AMP methods to the Z_2 and diatomics in the G2-1 set. The dissociation energies giving the positive ground state electron affinities for N_2 and H_2 were obtained from only the s-AMP method. [23,24]

3.0 Results:

Since 1967, this laboratory has evaluated experimental electron affinities and periodically selected the "best" values. [1, 2, 14, 50] In 2004, experimental electron affinities of organic molecules from donor acceptor complex absorption spectra, reduction potentials and gas phase E_a in exp-NIST, were examined for unreported systematic errors. [1,4] The only gas phase values with such errors were for biphenylene, 0.890 eV and p-t-amyl-nitro-benzene, 2.168 eV. The former was for an isochor, acenaphylene based on the agreement with the results for a chromatographically purified sample in the electron capture detector. The value for t-amyl-nitrobenzene was referenced to a gs-AE_a of nitrobenzene, 2 eV, now determined to be 1.008 eV. These findings were confirmed by CURES-EC.

The dipole bound electron affinities for the biologically significant tautomers of the nucleobases: (eV) A, 0.012(5); C, 0.085(8),0.230(8); U, 0.089(6); T, 0.069(8) were the only values listed in exp-NIST although we had reported gs-AE_a : (eV) A, 1.10(1); G, 1.58(1), C,1.05(1); U, 0.99(1); T, 0.98(1) from reduction potentials, chemical ionization negative ion mass spectra and onsets in literature NPES and confirmed them by CURES-EC. [1, 2] The exp-NIST database now includes vertical detachment energies E_{vd}: (eV) C, 2.34(10); U, 2.49(10); T, 2.40(10) assigned to valence states of rare tautomers.

The Hylleraas and CURES-EC were used to select gs-AE_a (Z and Z_2). This paper revisits values for Z_2 and extends the selection to diatomics in the G2-1 set. Newly assigned gs-E_a(Be & Mg) are 0.26 eV and gs-AE_a are: (eV) Cl_2, 3.2(2), Br_2, 2.87(14), CH, 2.1(2), H_2, 0.6, NH, 1.1, SiH, 1.9. The values for Be and Mg are from theoretical calculations and gs-E_a(B); the values for Cl_2 and Br_2 are from exp-NIST. The CH value is the average of values from exp-NIST and 1953R. [51-56] The values for H_2,NH and SiH are estimated from dN_{Hyl}. The anion dissociation energies are supported using semi-empirical anion Morse potentials, s-AMP.

3.1 The electron affinities of NO, O_2, and SF_6

The exp-NIST lists AE_a(NO):(eV) NPES-72, 0.024(10); NPES-89, 0.026(6); ECD-83,0.1(1); neutral beam-73, >0.1(1); electron impact, EI-69, >0.65(10); endothermic-76, 0.68(20); electron impact-68, 0.85(10); magnetron-64, 0.910647 and $AE_a(O_2)$:(eV) photodetatchment-58, 0.15(5); swarm-66, 0.43(2); EI-69 > 1.10(10); bracketing-70, 1.12(7); ion beam-70, > 1.27(20); NPES-71 to 03 , 0.430(30); 0.440(8); 0.451(7); 0.446(5) ECD-02, 0.725005. [4, 17, 30-44] The more precise spin orbital $AE_a(O_2)$, 0.450(2), 0.430(2) eV from the NPES-95 are not in exp-NIST. The 27 $AE_a(O_2)$, and 30 AE_a(NO) used to calculate the HIMPEC in figure. 1 are consistent with all the values in exp-NIST, peaks in the NPES-95 and the data from this laboratory and others plotted in Figures. 1, 3 and 4. The m/z = 30 and 32 ion yield curves from electron impact on NO_2 obtained simultaneously and the ECD data reported by Freeman before 1970 giving multiple values are especially significant.

In 1953, Pritchard reported that the AE_a(NO) was positive based on electron attachment studies and stated "it seems fairly certain that the electron affinity of the oxygen molecule is of the order of 20 kcal./mole, (sic 0.85 eV from the Born Haber Cycle) and that electron attachment, which takes place with almost zero exothermicity, leads to an excited state of O_2 which is stabilized either by collision or by radiation of the excess energy." [5] The PD-58-$AE_a(O_2)$ 0.15(5) eV and the magnetron-64, 0.910647 eV were the first precise AE_a to be reported. Then, Freeman determined $AE_a(O_2)$ 0.45 and 0.9 eV and AE_a(NO) 0.1 eV and 0.9 eV from the ECD data in Figure. 1. Since 1973, the $AE_a(O_2)$ 0.45 and AE_a(NO) 0.026 eV values have become the benchmark values. In 2003 this laboratory reported positive $AE_a(O_2)$ for 24 electronic states from the ECD-72, ECD-03 data and the NPES-95. The $AE_a(O_2)$, 0.725005 eV average of two ECD values, 0.700 eV and 0.750 eV is the only significantly different value added to NIST since the bracketing-70, $AE_a(O_2)$, 1.12(7) eV .

In 2013, the atmospheric pressure negative ion mass spectrometer , API-NIMS, ECD, PDECD and CV data in figures 1, 3 and 5 were used to report AE_a for the 27 bonding spin orbital superoxide states. In figure 3 are: the 1958 photodetachment data; the 1969 m/z, 30 and 32 ion yield curves from the electron impact of NO_2; the equilibrium constants obtained from the CV, electron impact and photon data and peaks in the NPES-95 and imagining negative ion photoelectron spectra, IPES-10 used to assign peaks in the NPES-02. The peaks lower than 0.1 eV are assigned to Efimov like states.

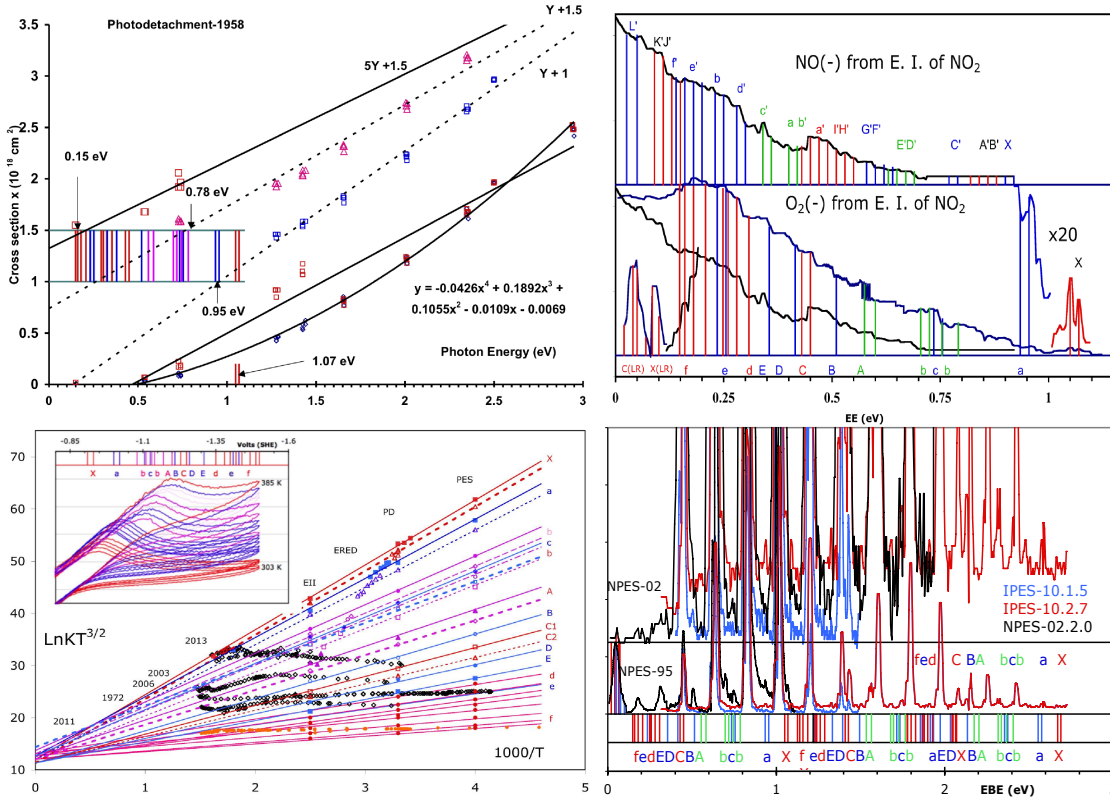

Fig. 3 Experimental data illustrating the identification, and assignment of valence state and long range electron affinities of oxygen: photodetachment-58 data from ref 30; electron impact data from ref. 33; CV and thermal data from refs. 14-18,23, 24, 30, 31 and photoelectron spectra from refs. 3,20,38,39. The X axes for all but the CV and thermal data are energies in eV and the Y axes are ion currents and cross sections in arbitrary units. The electron impact data ion yield of m/z =30 and 32 from the electron impact of NO_2 vs energy from ref. 33. The thermal data are plots of Ln $KT^{3/2}$ vs 1000/T. The CV are plots of current vs potential from ref. 23.

In 2003, Dinu, Groennboom and van der Zande reported 12 hyperfine energies of the $C\ ^2\Pi_{3/2,1/2}$ superoxide state from photodissociation above the $O(^2P_{3/2,1/2})$ + $O(^3P_{2,1,0})$ limits. [28] In 2010, Cavanagh and co-workers reported the first fully resolved peaks for the six hyperfine states of atomic oxygen anion shown in Figure 4. [29] The 12 resolved $C\ ^2\Pi_{3/2,1/2}$ peaks displaced by the fine structure, 20 meV and the 18 B, D, E, $^2\Sigma_{1/2}$ are lined up with the major peaks in the Kinetic Energy Release curve from Dinu et al. The identification of these 30 $C\ ^2\Pi_{3/2,1/2}$ hyperfine states suggest that the 54 spin orbital fine structure states should each be split into six giving a total of 6x54 = 324 hyperfine states. In Figures 5 and 6 are 162 hyperfine peaks at the positive hyperfine electron affinities in the cyclic voltammograms, electron impact, NPES-72, 95 and NPES-02. These are the first examples of both the fine and hyperfine structure levels for molecular anions suggested by Massey. These will be used to construct the first HIMPEC for hyperfine superoxide states.

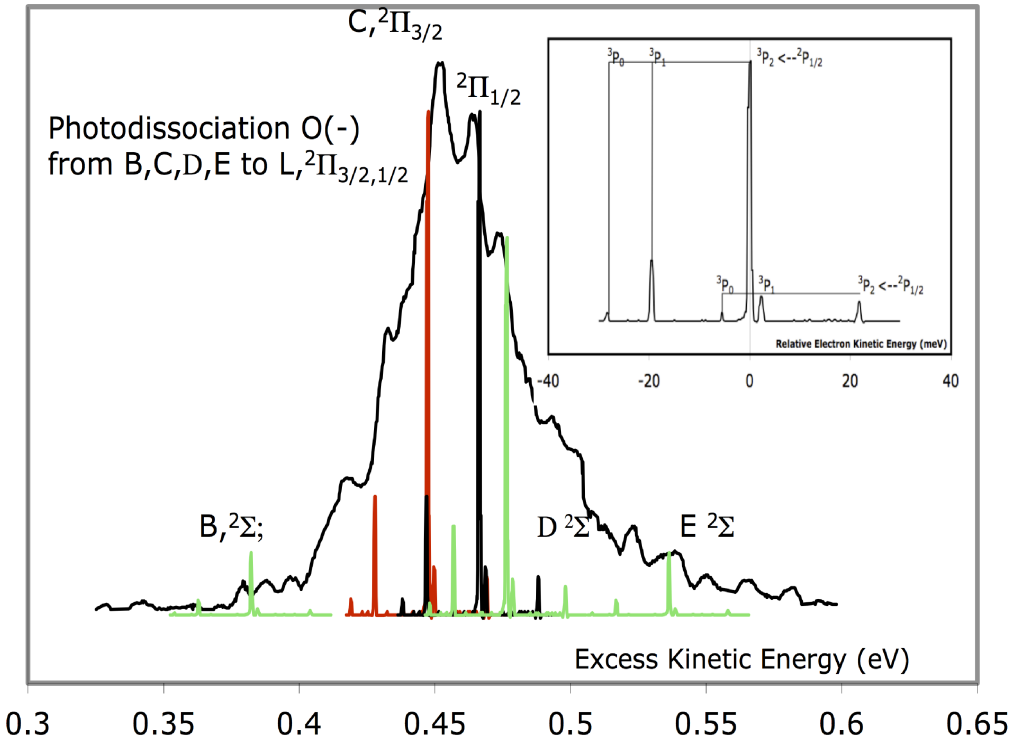

Figure 4 Photo dissociation data from reference 28 and hyperfine structure of O(-) from ref. 29. The atomic hyperfine structure separated by about 20 meV are lined up with the major peaks in the photodissociation curves demonstrating that the dominant dissociation occurs from the C state of superoxide. Also shown are minor peaks at the B, D, and E hyperfine states.

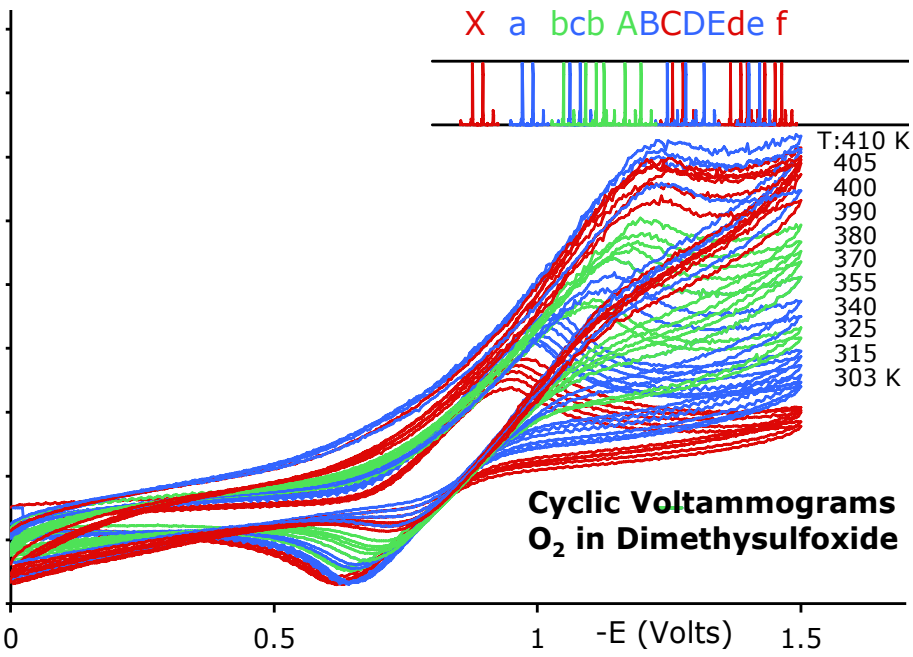

Figure 5 Hyperfine electron affinities of O_2 from cyclic voltammograms. The sources of the data and axes are given in Fig. 3 . The identification of the hyperfine state were carried out using the high resolution atomic data in Fig. 4.

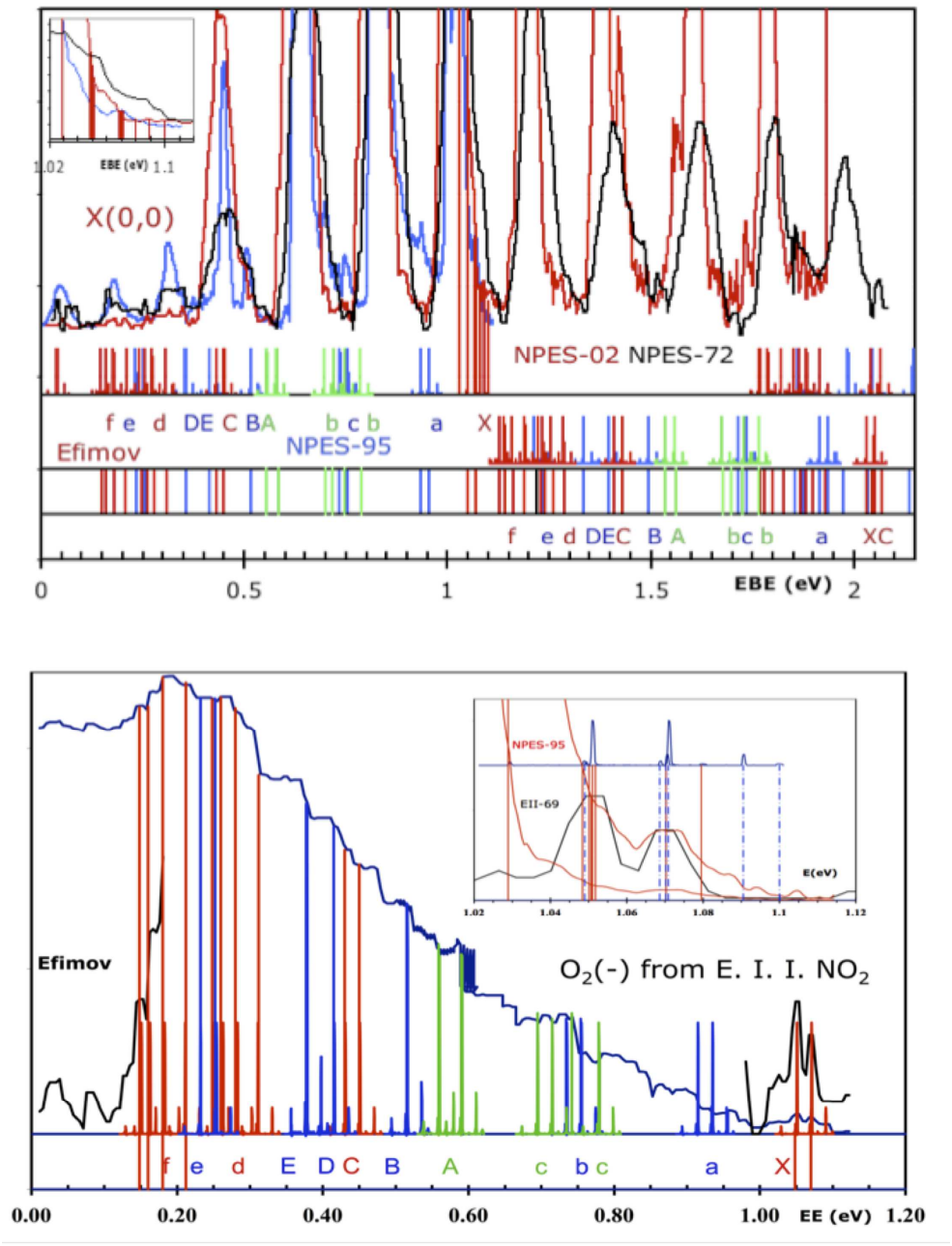

Figure 6 Hyperfine electron affinities of O_2 (top) from NPES-72, 95 and NPES-02 and (bottom) from m/z =32 from electron impact on NO_2. The sources of the data and axes are given in Fig. 3 . The identification of the hyperfine states were carried out using the high resolution atomic data in Fig. 4.

The deviation of the 2002R density functional $AE_a(SF_6)$: (eV) 1.67, 2.66, 2.83, 2.85, 3.00, 3.22 differ from the benchmark by at least 0.6 eV was described by the authors. "Perhaps the best experimental value for $EA(SF_6)$ is 1.07 (7) eV, as determined by Chen, Wiley, Batten, and Wentworth in 1994 using thermal electron attachment negative ion mass spectrometry. The DFT results […] severely overestimate this value by about 1.8 eV on average." [3] In 2007 we reported $AE_a(SF_6)$ from 0.15 eV to 2.6(2) eV from the temperature dependence of ECD, PDECD, API-NIMS, MGN, beam and swarm data and supported them by CURES-EC. Also, Jalbout and co-workers calculated theoretical $AE_a(SF_6)$ from 0.11 to 2.97 eV. We recently reported a new gs-$AE_a(SF_6)$, 3.0(1) eV, from surface ionization data collected by Pelc. The 2002R values clearly overlap this value and the E_{pd}, 3.16 eV reported in 1991. [47,48]

3.2 Electron affinities of atoms and homonuclear diatomics.

In 2013, we noted that the Hylleraas variational gs-AE_a(H), like the Rydberg is a fundamental constant. Hylleraas also calculated the first accurate atomic excited state electron affinities, 0.2876 eV for the metastable singly excited (2s) state of the hydrogen anion and lower values for doubly excited states. Following Efimov, there should be an infinite number of hydrogen anions with binding energies $0.75/(22.4)^n$ and $0.29/(22.4)^n$ analogous to Rydberg states of atoms. The E_a(H) per valence electron, designated the Hylleaas, Hyl = 0.75420375(3)/2 = 0.3771 eV/electron was used to select the first complete set of positive gs-AE_a($Z\&Z_2$) for the main group elements including the E_a(Pb), 1.1(1) eV assigned to the ground state in 1975 by Chen and Wentworth and electron affinities of the rare gases, N, Be , Mg, Zn, Cd, Hg. [8, 11,12] The exp-NIST experimental data base lists: (eV) C, 1.262114(44); Si, 1.389517(44); Ge, 1.232713(44); Sn, 1.112074(44); Pb, 0.365(8). The E_a(Pb) 0.365(8) is assigned to an excited state analogous to those of Si, 0.597, Ge, 0.401, Sn, 0.397. The remaining gs-E_a(Z) are the largest experimental values in exp-NIST. [4]

The 1953R noted that the N(-) ion had been observed in the gas phase. The 2002R listed AE_a(N): (eV) -0.32, 0.18, 0.30, 0.38, 0.60, 0.75 and AE_a(Be): (eV) -0.19, 0.31, -0.38, -0.25, -0.03, 0.27. The AE_a(N), 0.75 eV, equal to the AE_a(H) and AE_a(P) and the AE_a(Be), 0.29 eV equal to the AE_a(B) were assigned to the ground states. The NIST database of theoretical values, t-NIST lists only negative electron affinities for He, Ne, A, Zn, H_2, and N_2. The t-NIST also gives: (eV) AE_a(N) -8 to 0; 0 to 0.75; 0.75 to 3.0 and AE_a(Be) -6 to 0; 0 to 0.35; 0.35 to 1. The theoretical values larger than those for the ground state are overestimates and the negative values are assigned to excited states following Lesk and Efimov.

Except for O_2, and H_2, the benchmark $AE_a(Z_2)$ were assigned to the ground states. In 2004, Herder reproduced the benchmark AE_a for F_2, Cl_2, Br_2, and I_2 using CURES-EC. [21] The $AE_a(H_2)$, 0.38 eV (from dN_{Hyl} =-1) was assigned to the ground state in 2013. Here, the $AE_a(H_2)$, 0.6 eV, (from dN_{Hyl} = -0.5 and equal to the gs-$AE_a(N_2)$, 0.6 eV) is assigned to the ground state. The dissociation energies from the s-AMP give $AE_a(N_2)$, 0.6 eV and $AE_a(H_2)$, 0.6 eV. The exp-NIST lists multiple $AE_a(Cl_2)$ that overlap the benchmark, 2.38(10) eV ; VE_a ,1.02(5) eV and an alkali metal beam value of 3.20(20) eV and multiple $AE_a(Br_2)$ that overlap the benchmark 2.55 eV; VE_a 1.47 eV and an electron impact value of 2.87(10) eV. The largest values are assigned to the ground states. These assignments yield dN_{Hyl} (Cl_2) = (3.20-3.65)/0.377 = -1.19, and $dN_{Hyl}(Br_2)$ = (2.87- 3.36)/.377 = -1.29. The $dN_{Hyl}(I_2)$, -1.42 replaces the dN_{Hyl} (Cl_2) = (2.38-3.65)/0.377 = -3.37 as the smallest value. The $AE_a(Cl_2)$, 3.20(20) eV overlaps five DF values in 2002R. The new gs-$AE_a(Br_2)$ 2.87(10) eV is significantly lower than overestimates in 2002R and t-NIST. The dissociation energies from the s-AMP procedure support the new ground state values for Cl_2 and Br_2. The gs-AE_a for isoelectronic interhalogen diatomics are predicted to be comparable to the values for the homonuclear diatomics. The largest AE_a: (eV) FCl, 2.86(20); BrI, 2.70(20); ClI, 3.04 eV in exp-NIST, overlap the ground state values for Cl_2 and Br_2.

The $AE_a(S_2)$, 1.57(5) and > 2.5(8) eV in the exp-NIST overlap the benchmark gs-$AE_a(S_2)$,1.67(2) eV. The resulting dN_{Hyl} = (1.67-2.08)/.377= -1.09 overlaps the dN_{Hyl} for O_2 , F_2 , Cl_2 and Br_2. The 2002R gives density functional $AE_a(S_2)$:(eV) 1.64, 1.72, 1.82, 1.83, 2.27, 2.35. The last two are overestimates since these give positive dN_{Hyl}. The $AE_a(S_2)$ in the t-NIST, 0.584 to 1.7 eV can be assigned to multiple states analogous to O_2. The CURES-EC and s-AMP procedures support these assignments.

3.3 The electron affinities of the G2-1 diatomic hydrides and oxides.

The average AE_a(CH), 2.1(3) of the 2.6(3) eV in exp-NIST and 1.7(3) eV in the 1953R, is assigned to the ground state. The AE_a(CH), 1.238(8) eV and 0.74(5) eV in exp-NIST are assigned to excited states dissociating to C(-) +H and C + H(-). The 2002R cites density functional AE_a(CH): (eV), 0.72, 1.13, 0.75, 0.84, 1.33 that overlap these values. The benchmark AE_a(SiH), 1.277(9) eV is the only value in exp-NIST. The 2002R gives AE_a(SiH): (eV), 1.12, 1.17, 1.30, 1.49, 1.90, 1.90 and the t-NIST values from 0.4 to 3.3 eV. The density functional 1.90 eV is assigned to the ground state and the lower values to excited states by analogy to CH. The larger values in t-NIST are overestimates. The gs-AE_a of the isoelectronic GeH, SnH, PbH estimated to be about 2 eV by analogy to CH are confirmed by CURES-EC..

The only AE_a(NH), 0.370(4) eV in the exp-NIST corresponds to a dN_{Hyl}, -1 for dissociation to H(-) + N and N(-) + H. The 2002R lists AE_a(NH): (eV) -0.02, 0.45, 0.53, 0.63, 0.89, 1.21 and the t-NIST, values from 0 to 1.236 eV. The dN_{Hyl}, 1 gives a gs-AE_a(NH) 1.13 eV. The AE_a(PH), > 0.5(2) eV in exp-NIST with dN_{Hyl}(H/PH), -1 is assigned to an excited state. The gs-AE_a(PH), 1.028(1) eV in exp-NIST corresponds to a dN_{Hyl}(P/PH), 1. The 2002R lists AE_a(PH): (eV) 0.86, 1.02, 1.10, 1.59, 1.72 while the t-NIST gives values from 0 to 3.73 eV. The values greater than 1.028(1) eV are overestimates. The gs-AE_a of the isoelectronic AsH, SbH, BiH estimated to be about 1 eV by analogy to PH are confirmed by CURES-EC.

All of the AE_a (OH, SH) in the ex-NIST including the 1969 magnetron AE_a(OH), 1.89(12) eV and AE_a(SH), 2.298(39) eV overlap the benchmark AE_a(OH), 1.82767 eV and AE_a(SH), 2.317(2) eV. An error found in the exp-NIST values is the date of the 2000 AE_a(SH), 2.3182 eV listed as 1900. The 1953R lists Born Haber cycle AE_a (OH, SH) that overlap the benchmark. The benchmark values correspond to dN_{Hyl},(O/OH&S/SH) about 1. The largest AE_a for states dissociating to Z + H(-) are predicted to be about 0.75 + 0.377 = 1.1 eV based on the dN_{Hyl},(O/OH&S/SH) about 1. The 2002R lists AE_a(OH):(eV) 1.81, 2.29, 1.28, 1.92, 2.04, 2.80 and AE_a(SH): (eV) 2.38, 2.91, 2.13, 2.28, 2.49, 3.08 while the t-NIST cites positive values from near zero to 3.08. The values larger than the benchmarks are overestimates. The gs-AE_a of the isoelectronic SeH, 2.212525(44) eV and TeH, 2.10(2) eV are larger than the values for Se and Te. The electron affinities for SH, SeH, and TeH are confirmed by CURES-EC but not for OH. However, as in the case of superoxide, the anion dissociation energy for OH does reproduce the experimental gs-AE_a(OH).

The exp-NIST cites two values that overlap the benchmark AE_a(PO), 1.09(1) eV. The t-NIST cites values from 0 to 1.7 eV while the 2002R cites one value larger than the benchmark . The gs-AE_a(PO), 1.09(1) eV and the gs- AE_a(NO), 0.9 eV give dN_{Hyl}(O), -1 and dN_{Hyl}(N,P), 0.5. The AE_a(PO) in t-NIST and 2002R less than 1.1 eV can be assigned to excited state comparable to the values for the isoelectronic NO(-). The AE_a (PO) in t-NIST and 2002R greater than 1.1 eV are overestimates. The gs-AE_a of the isoelectronic AsO, SbO, BiO estimated to be about 1 eV by analogy to NO and PO are confirmed by CURES-EC.

3.4 The electron affinities of CN.

The exp-NIST lists three values that overlap the benchmark AE_a(CN), 3.682(4) eV , magnetron values 3.16124 and 2.8 eV and an AE_a(CN), 5.68(20) eV that contains a typographical error since the article lists only a value of 3.2(2) eV. The 2002R cites AE_a(CN): (eV), 4.04, 4.52, 4.04, 3.75, 3.88, 4.47 and the t-NIST -2.5 to 4.2. The values larger than the benchmark are overestimates while the values less than the benchmark, including the negative values can be assigned to excited states. The dN_{Hyl}(C/CN) = (3.682- 1.262)/0.377 = 6.42 is now the largest value for a diatomic surpassing the $dN_{Hyl}(C_2)$, 5.33. The difference between the MGN and benchmark value, 3.682-3.161 = 0.521eV is the same as the difference for the gs-E_a(C) –E_a(N) = 1.262-0.75 = 0.51 eV giving the same energy dissociating to C + N(-) as to C(-) + N. The gs-AE_a of the isoelectronic SiN, GeN, SnN, PbN estimated to be about 3.5 eV by analogy to CN are confirmed by CURES-EC.

3.5 Herschbach Ionic Morse Person Electron Curves.

In the 1960's, Herschbach calculated Morse potentials for diatomic halogen anions following W. B. Person. In his Nobel lecture, he recalled the classifications using the signs of the energy for dissociative electron attachment, E_{dea}, = $D_e(AB) - E_a(A \text{ or } B)$, VE_a and the $D_e[AB(-)]$ that resulted in some impossible cases since the $D_e[AB(-)]$ is always greater than zero. We replaced the $D_e[AB(-)]$ by the $AE_a[AB]$ to defines $2^3 = 8$ possible groups now designated Herschbach Ionic Morse Person Electron Curves, HIMPEC. [1,25,26] The neutral potentials and HIMPEC are:

$$U(AB) = D_e(AB)\text{-}2\, D_e(AB)\exp(-\beta(r - r_e)) + D_e(AB)\exp(-2\beta(r - r_e)) \quad (1)$$

$$U(AB^-) = D_e(AB)\text{-}2k_A D_e(AB)\exp(-k_B\beta\,(r\text{-}r_e)) + k_R D_e(AB)\exp(-2k_B\beta(r\text{-}r_e)) - E_a(B \text{ or } A) \quad (2)$$

$\beta = m_e(2\pi^2\mu/\, D_e[AB])^{1/2}$, μ, is the reduced mass, the r_e are the internuclear distance, r, at the minimum in the potentials. The HIMPEC are also Morse potentials with the parameters: $D_e(AB[-])/D_e(AB) = [k_A^2/k_R]$; $r_e(AB[-]) - r_e(AB) = [\ln(k_R/k_A)]/[k_B\,\beta(AB)]$; $\upsilon_e(AB[-])/\upsilon_e(AB). = [k_A k_B/k_R^{1/2}]$. The E_a, VE_a and E_{dea} and /or other data give the dimensionless constants k_A, k_B and k_R.

The present evaluation methods were used to report the electron affinities of NO and O_2 illustrated by HIMPEC in Figure 1. Dinu and co-workers identified 12 hyperfine states of superoxide from the competition between photodetachment and photodissociation from only the v =0 levels of the $^2\Pi_{3/2,1/2}$, C state. The HIMPEC for the hyperfine X $^2\Pi$, $A^2\Delta$, B $^2\Sigma$, C $^2\Pi$, D $^2\Sigma$, E $^2\Sigma$, and f4 $^4\Pi$ states from the $AE_a(O_2)$ are referenced to zero at infinite separation while those in Figure 1 are referenced to the zero at the internuclear distance of the neutral. The Morse parameters assumed to be the same for each of the hyperfine states dissociate to the atomic hyperfine limits separated by 0.05 eV for each spin state.

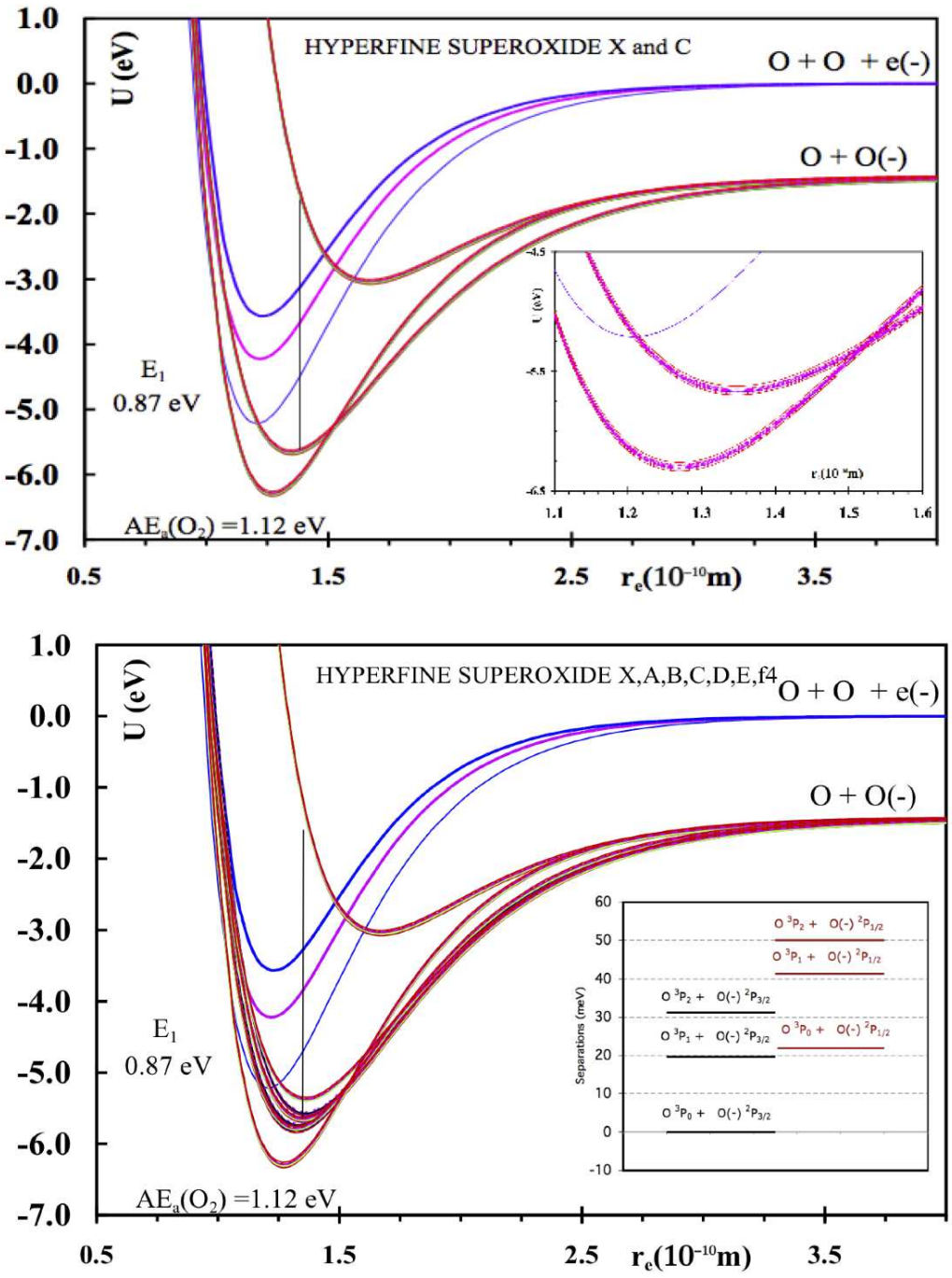

Figure 7 HIMPEC for hyperfine X $^2\Pi$, A$^2\Delta$, B $^2\Sigma$, C $^2\Pi$, D $^2\Sigma$, E $^2\Sigma$, and f4 $^4\Pi$ states and the antibonding I4 state leading to the photodissociation data given by Dinu and co-workers in ref. 28. The lower inset is an expansion of the six limits from Ref. 29. These curves can be compared to those in Fig. 1 showing the 54 spin orbital states.

At present it is generally assumed that H_2 and N_2 cannot form valence state anions more stable than the neutral, even at very low temperatures. However, this is not supported by the quantum mechanical theorem presented by Lesk. The parameters for the bonding anions of H_2 and N_2 were obtained using s-AMP. The bonding HIMPEC for $H_2(-)$ and $N_2(-)$ shown in Fig. 6 are to our knowledge the first such Morse potentials. The bonding curve for $N_2(-)$ is calculated from parameters obtained from the s-AMP PM3(5200) calculation that also gives an $AE_a(N)$, 0.75 eV in agreement with the largest density functional value in the 2002R. Also shown are curves giving an $AE_a(N_2)$, slightly larger than zero. This corresponds to an Efimov like state dissociating to a limit of N + N + e(-) or N + N(-). The antibonding curve calculated by Flores from electron scattering data in 1985 was published in his Master's thesis entited "Negative Ion States for $H_2(-)$ and the second row homonuclear diatomics" [56]

Brandon Jordon-Thaden and co-workers recently observed long lived anions of H_2, and D_2 with two distributions, one due to dissociation and one due to detachment reminiscent of the work by Dinu and co-workers on superoxide. Srivastava and co-workers have calculated ab-initio curves for $H_2(-)$ and summarized the earlier work. [57, 58] A more detailed discussion of the vast amount of theoretical and experimental work on the characterization of $H_2(-)$ is clearly beyond the scope of this article. However, the support for the existence of multiple anion states is clearly pertinent. Flores calculated antibonding HIMPEC for $H_2(-)$ using data published before 1985 including the $AE_a(H_2)$, -1 eV. [58] The long range state with a small positive $AE_a(H_2)$ is an Efimov like state. The s-AMP procedure yields a maximum dissociation energy for $H_2(-)$, 4.6 eV that gives a gs-$AE_a(H_2)$, 0.6 eV. The bonding HIMPEC for $H_2(-)$ uses the s-AMP parameters with a smaller internuclear distance to provide a "back-side crossing of the anion and neutral.

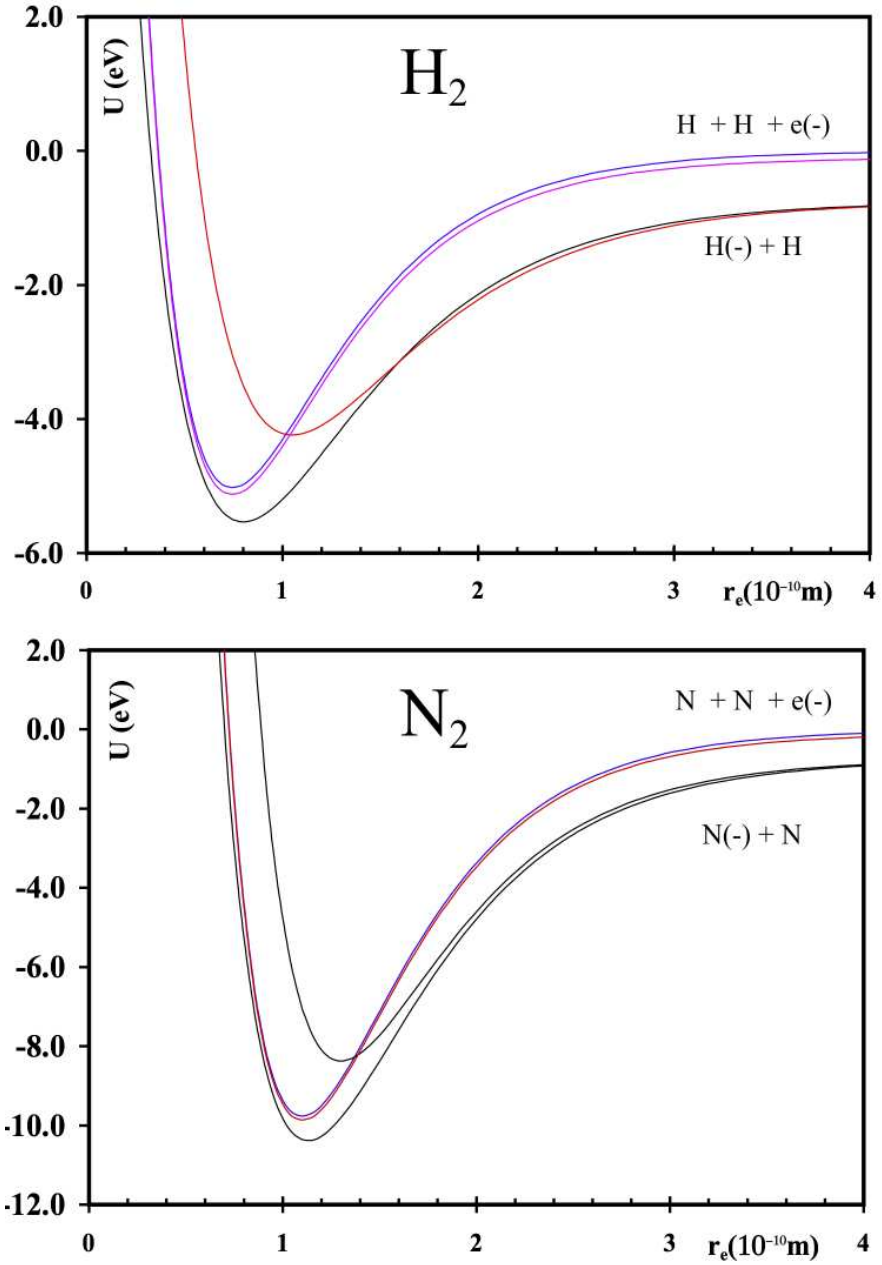

Fig. 8 Neutral and anion Morse potentials for H_2 and N_2 calculated from dissociation energies for anions for both from the s-AMP method, from long range positive electron affinities for both following Efimov. The CURES-EC electron affinity of N_2 is 0.6 eV.

4.0 Conclusions and future work

The major conclusion of this work is that there are a multitude of negative ion states with positive electron affinities so that theoretical electron affinities should be compared to more than one benchmark. The three body Z(+) + 2e(-) and A + B + e(-) systems support an infinite number of stable anions following Efimov, and the limit to the gs-electron affinity is zero following Lesk. For di and polyatomic anions, the limit to the anion dissociation energy is zero allowing for negative excited state electron affinities such as for $SF_n(-)(n=1-6)$, the nucleobase anions and other organic molecules evaluated by this laboratory. Other conclusions are:

(a) the gs-AE_a shown in Table 3 are the largest experimental values: (eV) O_2,1.120(5), S_2,1.67(2); F_2, 3.08(7), Cl_2, 3.2(2); Br_2, 2.87(14); CH, 2.1(2); OH, 1.82767, SH, 2.317(2); PH, 1.028(1); CN, 3.682(4); NO, 0.93(1); PO, 1.09(1); SF_6,3.0(2) or the largest predicted AE_a : (eV) N, 0.75; H_2, 0.6 ; N_2, 0.6; NH, 1.1, SiH, 1.90.

(b) theoretical electron affinities in Table 3 larger than the ground state value are overestimates

(c) the gs-AE_a of isoelectronic species can be predicted from the above values

(d) multiple electron affinities predicted by electron correlation rules can be accurately reproduced by theoretical methods.

The present work can be extended to other polyatomic molecules. The 2002R lists five density functional AE_a for 15 atoms, including N, Cl and Br, and 108 molecules compared to one experimental benchmark and five density functional AE_a for one atom, Be, and 41 molecules without any benchmarks. The gs-AE_a of the 16 atoms, 11 diatomics and SF_6 in 2002R, were assigned in this article. This leaves many other density functional values to be considered. The exp-NIST contains multiple AE_a of many species that should be used as benchmarks for theoretical calculations. A paper identifying all of the positive hyperfine $AE_a(O_2)$ has recently been accepted for publications. [59]

References

1. Chen ES, Chen ECM *The Electron Capture Detector & Thermal Electron Reactions* Wiley, 2004.
2. Chen ES, Chen ECM , (2007) Electron affinities and activation energies for reactions with thermal electrons: SF_6 and SF_5, Phys Rev A76: 032508.
3. Rienstra-Kiracofe JC, Tschumper GS, Schaefer HF, Nandi S, Ellison GB (2002) Atomic and molecular electron affinities: Photoelectron experiments and theoretical computations. Chem Rev 102: 231-282.
4. National Institute of Standards and Technology (NIST) Chemistry WebBook, [http://webbook.nist.gov/ and Cccbdb.nist.gov/ (accessed 2013).
5. Pritchard HO (1953) The determination of electron affinities Chem Rev 52:529-563.
6. Massey, HSW (1950) *Negative Ions* Cambridge University Press.
7. Lesk, AM (1968) Use of the Hartree Fock pproximationin calculating electron affinities. Phys Rev 171: 7-10.
8. Efimov V (1970) Energy levels arising from resonant two-body forces in a three-body system. Phys Lett B 33:563-564.
9. Berry RS (1969) Small free negative ions. Chem Rev 69: 533-542.
10. Wildt R (1939) Electron affinity in astrophysics. Astrophysical Journal 89: 295-301
11. Hylleraas, EA (1950) A new stable state of the negative hydrogen ion. Astrophysical Journal 111:209-213.
12. Hylleraas, EA (1964) The negative hydrogen ion in quantum mechanics and astrophysics. Astrophysica Norvegica 9: 345-349.
13. Bethe, HM http://www.webofstories.com/play/4483, accessed 7/7/2012.
14. Chen ES, Chen ECM (2013) The Hylleraas binding energy of hydride and electron affinities. J Theor Comp Chem 12:1350016
15. Chen ES, Herder C, Keith H, Chen ECM (2010) Hund's strong field states of superoxide and NO(-). J Theor Comp Chem 9: 1-8.
16. Freeman, RR (1971) I. Electron attachment to selected small molecules: II The development and charcterization of a photoionization/electron capture detector for use in gas chromatography systems. Doctoral dissertation, University of Houston.
17. Chen ES, Chen ECM (2003) Semiempirical characterization of homonuclear diatomic ions: 6. group VI and VII anions. J Phys Chem A 107:169-177.
18. Chen ECM , Herder C, Chang S, Ting R, Chen ES (2006) Experimental determination of spin–orbital coupling states of $O_2(-)$. J Phys B 39: 2317-2333.
19. Jalbout AF, De Leon A, Adamowicz L, Trzaskowski B, Chen ECM, Herder C, Chen ES, (2007) Theoretical, empirical and experimental electron affinities of SF_6: Solving the density functional enigma. J Theor Comp Chem 6: 747-759.
20. Schiedt H, Weinkauf R (1995) Spin orbital coupling in superoxide. Z Naturforsch 50a:1041-1045.
21. Herder C (2005) Experimental and theoretical determination of fundamental properties of molecular oxygen and other atmospheric molecules using the pulsed discharge electron capture detector and semi- empirical quantum mechanical calculations. Siemens application, available on request.
22. Toader EI, Graham WG (2008) Transient induced molecular negative ions formed in cold electron collisions with polarized molecules Nukleonika 53:123-126
23. Pai S (2010) Experimental and theoretical determination of fundamental properties of molecular oxygen and other atmospheric molecules using the pulsed discharge electron capture detector and semi-empirical quantum mechanical calculations. Siemens application available on request.
24. Pai S, Anderson C, Chen ES, Chen ECM, (2011) What are the 54 electron affinities of O_2, Molecular Structure 23:407-410

25. Herschbach DR (1987) Molecular dynamics of elementary chemical reactions (Nobel Lecture). Angew Chem Int Ed Engl 26:1221-1243.
26. Person WB (1963) Electron affinities of some halogen molecules and the charge-transfer frequency J Chem Phys 38: 109-116.
27. Khuseynov D, Fontana M, Sanov A, (2012) Photoelectron spectroscopy and photochemistry of tetracyanoethylene radical anion in the gas phase. Chem Phys Letters 550:15-18.
28. Dinu L, Gerrit C, Groenenboom Wim J. van der Zande (2003) Vibronic coupling in the superoxide anion: The vibrational dependence of the photoelectron angular distribution. J Chem Phys 119:8865-8872.
29. Cavanagh SJ, Gibson ST, Lewis BR (2010) Photodetachment of O^- from threshold to 1.2 eV electron kinetic energy using velocity-map imaging. Journal of Physics: Conference Series 212: 012034
30. Burch DS, Smith SJ , Branscomb LM (1958) Photodetachment of O_2^-. Phys Rev 112: 171-175.
31. Pack JL, Phelps AV (1966) Electron attachment and detachment. I. Pure O_2 at low energy. J Chem Phys 44: 1870-1883.
32. Page FM , Goode GC (1969) *Negative ions and the magnetron*, Wiley-Interscience.
33. Stockdale JAD, Compton RN, Hurst GS, Reinhardt PW (1969) Collisions of monoenergetic electrons with NO_2: Possible lower limits to electron affinities of O_2 and NO. J Chem Phys 50: 2176-2180.
34. Siegel MW, Celotta RJ, Hall JL, Levine J, Bennett RA (1972) Molecular Photodetachment Spectroscopy. I. The electron affinity of nitric oxide and the molecular constants of NO^-. Phys Rev A 6: 607-631.
35. Williams JM, Hamill WH (1968) Ionization potentials of molecules and free radicals and appearance potentials by electron impact in the mass spectrometer J Chem Phys 49: 4467-4477.
36. Bailey TL, Mahadevan P (1970) Electron transfer and detachment in collisions of low-energy negative ions with O_2. J Chem Phys 52:179-190.
37. Vogt D, Hauffle B, Neuert H (1970) Ladungsaustausch-reaktionen einiger negativer ionen mit O_2 und die elektronenaffinitat des O_2. Z Phys 232: 439-444.
38. Celotta RJ, Bennett RA , Hall JL, Levine J, Siegel MW (1971) Electron affinity of O_2 by laser photodetachment, Bull Am Phys Soc 16: 212.
39. Celotta RJ, Bennett RA , Hall JL, Siegel MW, Levine J (1972) Molecular Photodetachment Spectrometry. II. The electron affinity of O_2 and the structure of O_2^- Phys Rev A 6: 631-641.
40. Shimamori H, Fessenden RW (1981) Thermal electron attachment to oxygen and van der Waals molecules containing oxygen, J Chem Phys 74: 453-467.
41. Gooding JM, Hayhurst AN (1987) Kinetics of electron attachment to oxygen and water in Flames, Nature 281: 204 – 206.
42. Caspar H, Tiedje J (1980) Response of electron-capture detector to hydrogen, oxygen, nitrogen, carbon dioxide, nitric oxide and nitrous oxide J Chromatogr 193:142-146.
43. Travers MJ, Cowles DC, Ellison GB (1989) Reinvestigation of electron affinities of O_2 and NO, Chem Phys Lett 164:449-455.
44. Ervin KM, Anusiewicz I, Skurski P, Simons J, Lineberger WC (2003) The only stable state of O_2^- Is the $X\ ^2\Pi_g$ ground state and it (Still!) has an adiabatic electron detachment energy of 0.45 eV, J Phys Chem A 107:8521-8529.
45. Le Garrec J, Sidko O, Queffelec J, Hamon S, Mitchell J, Rowe B (1997) Experimental studies of cold electron attachment to SF_6 , CF_3Br , and CCl_2F_2 .J Chem Phys 107: 54-63.
46. Chen ECM, Shuie LR, D'sa, ED, Batten C, Wentworth WE (1988) Negative ion states of sulfur hexafluoride. J Chem Phys 88:4711-4719.

47. Datskos PG, Carter JG, Christophorou LG (1995) Photodetachment of SF_6^- .Chem Phys Lett 239: 38-43.
48. Pelc A (2012) Generation of negative ions from SF_6 gas by means of hot surface ionization Rapid Communications in Mass Spectrometry 26: 577-580.
49. Chen ES, Chen ECM (2013) Negative surface ionization electron affinities and activation energies of SF_n Rapid Communications in Mass Spectrometry 27: 577-582.
50. Chen ECM, Wentworth W E (1975) The experimental values of atomic electron affinities: Their selection and periodic behavior J Chem Ed 52:486-489.
51. Lacmann K, Herschbach DR (1970) Collisional excitation and ionization of K atoms by diatomic molecules: The role of ion pair states Chem Phys Lett 6: 106-110.
52. DeCorpo JJ, Franklin JL (1971) Electron affinities of the halogen molecules by dissociative electron attachment J Chem Phys 54: 1885-1888.
53. Locht R, Momigny J (1970) Mass spectrometric determination of electron affinities of radicals Chem Phys Lett 6: 273-276.
54. Smith LG (1937) Ionization and dissociation of polyatomic molecules by electron impact. I. methane Phys Rev 51:263-275.
55. Shiell RC, Hu XK, Hu QJ, Hepburn JW (2000) Threshold ion-pair production spectroscopy (TIPPS) of H_2 and D_2 J Phys Chem A 104: 4339-4342.
56. Flores, RA "Negative ion states for H_2(-) and the second row homonuclear diatomics" Masters thesis University of Houston Clear Lake, 1985
57. Kreckel1 H, Herwig P, Schwalm D, Cızek M, Golser R, Heber O, Jordon-Thaden B, Wolf A (2014) Metastable states of diatomic hydrogen anions Journal of Physics: Conference Series 488: 012034.
58. Srivastava S, Sathyamurthy N, Varandas AJC (2012) An accurate ab initio potential energy curve and the vibrational bound states of H_2^- Chemical Physics 398: 160–167.
59. Chen ES, Pai S, Chen ECM, (2014 accepted for publication) Hyperfine electron affinities of molecular oxygen, Computational and Theoretical Chemistry

Attributions: The Morse potentials for N_2 and H_2 anions were calculated using HIMPEC procedures developed by Flores for the diatomic anions of the second row atoms. The PDECD data and development of the CURES-EC method were carried out by Herder. The development of s-AMP method and the collection of the cyclic voltammetry data were carried out by Pai. The new applications of the theoretical methods were carried out by Pham, Lim, Rosenthal. Herder, Pai, Lim, Rosenthal and Pham were Wentworth Scholars and Lim and Rosenthal were HYPERCHEM Scholars who conducted research under the direction of Chen, Chen, and Keith. The paper was written by the latter and has been examined by all of the authors. The support of Hypercube and the Wentworth Foundation is appreciated by the authors.

Table 1 Oxygen: Activation energies, E_1 , dN_{Hyl} and Electron Affinities, E_a

State	E_1 (eV)	AE_a (eV)	dN_{Hyl}	State	E_1 (eV)	AE_a[a] (eV)	dN_{Hyl}
X1 $^2\Pi_{3/2}$	0.89	1.070(2)	[-1.00]	F1 $^2\Pi_{3/2}$	1.6	-1.62	[-8.00]
X2 $^2\Pi_{1/2}$	0.87	1.050(2)	-1.08	F2 $^2\Pi_{1/2}$	1.6	-1.64	-8.22
a1-$^4\Sigma^-_{3/2}$	0.84	0.960(2)	-1.33	g1-$^4\Sigma^-_{3/2}$	1.7	-1.75	-8.51
a2-$^4\Sigma^-_{1/2}$	0.82	0.940(2)	-1.38	g2-$^4\Sigma^-_{1/2}$	1.7	-1.77	-8.56
b1-$^4\Delta_{7/2}$	0.68	0.787(2)	-1.78	h1-$^4\Delta_{7/2}$	1.9	-1.92	-8.97
b2-$^4\Delta_{5/2}$	0.68	0.751(2)	-1.88	h2-$^4\Delta_{5/2}$	1.9	-1.97	-9.07
b3-$^4\Delta_{3/2}$	0.68	0.725(2)	-1.94	h3-$^4\Delta_{3/2}$	1.9	-1.99	-9.13
b4-$^4\Delta_{1.2}$	0.66	0.705(2)	[-2.00]	h4-$^4\Delta_{1.2}$	2.0	-2.01	[-9.00]
c1-$^4\Sigma_{3/2}$	0.68	0.755(2)	-1.87	i1-$^4\Sigma_{3/2}$	2.0	-1.96	-9.06
c2-$^4\Sigma_{1/2}$	0.68	0.735(2)	-1.92	i2-$^4\Sigma_{1/2}$	2.1	-1.98	-9.10
A1-$^2\Delta_{5/2}$	0.48	0.601(1)	-2.28	G1-$^2\Delta_{5/2}$	2.1	-2.11	-9.46
A2-$^2\Delta_{3/2}$	0.48	0.561(1)	-2.38	G2-$^2\Delta_{3/2}$	2.1	-2.15	-9.57
B-$^2\Sigma_u$	0.27	0.515(2)	-2.50	H-$^2\Sigma_u$	2.2	-2.20	-9.69
C1-$^2\Pi_{3/2}$	0.13	0.450(2)	-2.67	I1-$^2\Pi_{3/2}$	2.3	-2.26	-9.86
C2-$^2\Pi_{1/2}$	0.13	0.430(2)	-2.73	I2-$^2\Pi_{1/2}$	2.3	-2.28	-9.91
D-$^2\Sigma_{1/2}$	0.12	0.415(2)	-2.78	J- $^2\Sigma_{1/2}$	2.3	-2.29	-9.92
E-$^2\Sigma_{1/2}$	0.12	0.355(2)	-2.93	K-$^2\Sigma_{1/2}$	2.4	-2.35	-10.11
d1-$^4\Pi_{5/2}$	0.12	0.312(2)	[-3.00]	j1-$^4\Pi_{5/2}$	2.4	-2.41	[-10.00]
d2-$^4\Pi_{3/2}$	0.10	0.280(2)	-3.13	j2-$^4\Pi_{3/2}$	2.4	-2.44	-10.43
d3-$^4\Pi_{1/2}$	0.10	0.260(2)	-3.18	j3-$^4\Pi_{1/2}$	2.5	-2.46	-10.39
d4-$^4\Pi_{-1/2}$	0.10	0.248(2)	-3.21	j4-$^4\Pi_{-1/2}$	2.5	-2.47	-10.44
e1-$^4\Sigma_{3/2}$	0.08	0.252(2)	-3.20	k1-$^4\Sigma_{3/2}$	2.5	-2.46	-10.39
e2-$^4\Sigma_{1/2}$	0.08	0.232(2)	-3.26	k2-$^4\Sigma_{1/2}$	2.5	-2.48	-10.48
f1-$^4\Pi_{5/2}$	0.08	0.212(2)	-3.31	l1-$^4\Pi_{5/2}$	2.6	-2.50	-10.50
f2-$^4\Pi_{3/2}$	0.08	0.180(2)	-3.39	l2-$^4\Pi_{3/2}$	2.6	-2.53	-10.58
f3-$^4\Pi_{1/2}$	0.07	0.160(2)	-3.44	l3-$^4\Pi_{1/2}$	2.6	-2.55	-10.63
f4-$^4\Pi_{-1/2}$	0.07	0.148(2)	[-3.50]	l4-$^4\Pi_{-1/2}$	2.6	-2.56	[-10.50]

a. The negative AE_a are calculated using the assumed dN_{Hyl} in brackets and the positive AE_a The NIST database of theoretical values http://cccbdb.gov.nist/ lists: 1.008 eV to -1.964 eV. The closest values for the doublet antibonding states are: (eV) -1.585, -1.603, -1.964. A curve for a doublet state with an AE_a; -3.39 eV and a double minimum curve for a quartet state with AE_a -1.8 eV and -2.40 eV are reported in Ref. 44.

Table 2: Nitric Oxide: CURES-EC and experimental electron affinities (eV)

	E_a	E_a(CEC)	MCCI	E_a (thermal)	E_a (other)
X,$^3\Sigma$	0.92	0.93	PM3(61UU)t	0.92	0.90
a,$^1\Delta$	0.40	0.40	PM3(3222)s	0.40	0.40
b,$^1\Sigma$	0.16	0.18	PM3(4122)s	0.15	0.17
A',B',$^3\Pi$	0.86	0.86	PM3(6122)t	0.86	0.86
A',B',$^3\Pi$	0.84	0.84	PM3(5100)t	0.85	0.85
A',B',$^3\Pi$	0.82	0.82	PM3(5122)t	0.83	0.80
C',$^3\Sigma$	0.75	0.70	PM3(4100)t	0.75	0.77
D',E',$^3\Delta$	0.67	0.68	PM3(4122)t	0.65	0.68
D',E',$^3\Delta$	0.65	0.68	PM3(4122)t	0.65	0.68
D',E',$^3\Delta$	0.63	0.62	PM3(UU00)t	0.63	0.65
F',$^3\Sigma$	0.62	0.62	PM3(UU00)t	0.63	0.60
G',$^3\Sigma$	0.58	0.60	PM3(0000)t	0.60	0.57
H',I',$^3\Pi$	0.53	0.51	PM3(0022)t	0.50	0.57
H',I',$^3\Pi$	0.51	0.51	PM3(0022)t	0.50	0.57
H',I',$^3\Pi$	0.49	0.51	PM3(0022)t	0.50	0.46
a' $^1\Pi$	0.45	0.43	PM3(6200)s	0.45	0.46
b' $^1\Pi$	0.43	0.43	PM3(6200)s	0.45	0.40
c',$^1\Delta$	0.35	0.35	PM3(6222)s	0.35	0.40
d',$^1\Sigma$	0.29	0.30	PM3(3200)s	0.27	0.27
e',$^1\Sigma$	0.25	0.22	PM3(3222)s	0.25	0.27
f',$^1\Sigma$	0.20	0.19	PM3(4100)s	0.20	0.17
J',K',$^3\Pi$	0.14	0.11	PM3(3100)t	0.11	0.10
J',K',$^3\Pi$	0.12	0.11	PM3(3100)t	0.10	0.10
J',K',$^3\Pi$	0.10	0.11	PM3(3100)t	0.08	0.10
L',$^3\Sigma$	0.026	0.04	PM3(3122)t	0.05	0.026

Table 3: Assigned ground state electron affinities and density functional values(eV)

	gs-AE_a	largest Exp	best t-NIST non-DF	R-2002 Density Functional B3LYP	B3P86	BHLYP	BLYP	BP86	LSDA
H	0.75419	0.75419	0.728(CCSD-T)	0.84	1.31	0.62	0.75	0.93	1.23
Be	0.29	0+	0.890(MP2-SDD)	-0.19	0.31	-0.38	-0.25	-0.03	0.27
N	0.75	-0.07	0.75(avg of several)	0.18	0.60	-0.32	0.30	0.38	0.75
H_2	0.6	0+	-	-	-	-	-	-	-
N_2	0.6	0+	-	-	-	-	-	-	-
O_2	1.120(5)	1.120	0.498(CBS-Q)	0.63	1.06	0.36	0.62	0.65	1.08
S_2	1.67(2)	1.67(2)	1.68(G4)	1.82	2.32	1.72	1.64	1.83	2.27
F_2	3.08(7)	3.08(7)	3.07(multiple)	3.77	4.10	3.56	3.72	3.67	3.84
Cl_2	3.2(2)	3.2(2)	2.99(MP2)	3.27	3.69	3.13	3.16	3.23	3.42
Br_2	2.87(14)	2.87(14)	2.87(avg of several)	3.12	3.56	3.02	2.97	3.07	3.29
CH	2.1(2)	2.1(2)	1.279(MP2-aug-cc-pVQZ)	1.36	1.94	1.06	1.33	1.59	2.13
SiH	1.90	1.277(9)	1.24(G4)	1.30	1.90	1.15	1.17`	1.49	1.90
NH	1.13	0.370(4)	0.355(G4)	-0.02	0.45	0.53	0.63	0.89	1.21
PH	1.028(1)	1.028(1)	1.02(CBS-Q)	1.10	1.59	0.86	1.02	1.20	1.72
OH	1.82767	1.82767	1.83(avg of several)	1.81	2.29	1.28	1.92	2.04	2.80
SH	2.317(2)	2.317(2)	2.38(CBS-Q)	2.38	2.91	2.13	2.28	2.49	3.08
CN	3.682(4)	3.682(4)	3.68(avg of several)	4.04	4.52	4.04	3.75	3.88	4.47
NO	0.93(1)	0.93(1)	0.467(MP2)	0.53	0.97	0.36	0.43	0.52	0.96
PO	1.09(1)	1.09(1)	1.09 (G3)	0.45	0.95	0.24	0.95	1.16	1.53
SF_6	3.0(2)	3.0(2)		2.66	2.83	1.61	3.22	3.00	2.85

The theoretical values larger than the ground state value are overestimates. The negative values are for excited states.

Figure Captions

Fig. 1: Neutral and anionic one dimensional Morse potential energy curves of energy vs internuclear separation referenced to the neutral dissociation energy = 0 and thermal data for NO and O_2 plotted as Ln $KT^{3/2}$ vs 1000/T from refs. 14-18,21,31,32,41,42.

Fig. 2: PDECD equipment used by Herder in 2004 from refs. 2,17,21.

Fig. 3 Experimental data illustrating the identification, and assignment of valence state and long range electron affinities of oxygen: photodetachment-58 data from ref 30; electron impact data from ref. 33; CV and thermal data from refs. 14-18,23, 24, 30, 31 and photoelectron spectra from refs. 3,20,38,39. The X axes for all but the CV and thermal data are energies in eV and the Y axes are ion currents and cross sections in arbitrary units. The electron impact data ion yield of m/z =30 and 32 from the electron impact of NO_2 vs energy from ref. 33. The thermal data are plots of Ln $KT^{3/2}$ vs 1000/T. The CV are plots of current vs potential from ref. 23.

Fig. 4: Photo dissociation data from reference 28 and hyperfine structure of O(-) from reference 29. The atomic hyperfine structure separated by about 20 meV are lined up with the major peaks in the photodissociation curves demonstrating that the dominant dissociation occurs from the C state of superoxide. Also shown are minor peaks at the B, D, and E hyperfine states.

Fig. 5: Hyperfine electron affinities of O_2 from cyclic voltammograms. The sources of the data and axes are given in Fig. 3 . The identification of the hyperfine state were carried out using the high resolution atomic data in Fig. 4.

Fig: 6 Hyperfine electron affinities of O_2 (top) from NPES-72, 95 and NPES-02 and (bottom) from m/z =32 from electron impact on NO_2. The sources of the data and axes are given in Fig. 3 . The identification of the hyperfine states were carried out using the high resolution atomic data in Fig. 4.

Fig. 7: HIMPEC for hyperfine X $^2\Pi$, A $^2\Delta$, B $^2\Sigma$, C $^2\Pi$, D $^2\Sigma$, E $^2\Sigma$, and f4 $^4\Pi$ states and the antibonding I4 state leading to the photodissociation data given by Dinu and co-workers in ref. 28. The lower inset is an expansion of the six limits from Ref. 29. These curves can be compared to those in Fig. 1 showing the 54 spin orbital states.

Fig. 8: Neutral and anion Morse potentials for H_2 and N_2 calculated from dissociation energies for anions for both from the s-AMP method, from long range positive electron affinities for both following Efimov. The CURES-EC electron affinity of N_2 is 0.6 eV.